J. Fluid Mech. (2014), *vol.* 744, R2, doi:10.1017/jfm.2014.94

JFM RAPIDS
journals.cambridge.org/rapids

On the lifetimes of evaporating droplets

J. M. Stauber[1], S. K. Wilson[1,†], B. R. Duffy[1] and K. Sefiane[2]

[1]Department of Mathematics and Statistics, University of Strathclyde, Livingstone Tower, 26 Richmond Street, Glasgow G1 1XH, UK

[2]School of Engineering, University of Edinburgh, The King's Buildings, Mayfield Road, Edinburgh EH9 3JL, UK

(Received 19 December 2013; revised 7 February 2014; accepted 16 February 2014)

The complete description of the lifetime of a droplet on a solid substrate evaporating in a 'stick–slide' mode is obtained. The unexpectedly subtle relationship between the lifetime of such a droplet and the lifetimes of initially identical droplets evaporating in the extreme modes (namely the constant contact radius and constant contact angle modes) is described and summarised in an appropriate master diagram. In particular, it is shown that the lifetime of a droplet is not, in general, constrained by the lifetimes of the extreme modes.

Key words: condensation/evaporation, phase change

1. Introduction

The evaporation of droplets on solid substrates is not only of fundamental scientific interest but also of importance in a wide variety of practical applications, such as pesticide spraying, DNA micro-array analysis, inkjet printing, microfabrication and spray cooling. In particular, optimising the lifetimes of evaporating droplets may allow considerable efficiencies and economies to be achieved in a variety of industrial contexts. The recent review articles by Cazabat & Guéna (2010) and Erbil (2012) give excellent overviews of the diverse and rapidly expanding literature on droplet evaporation.

The lifetime of an evaporating droplet depends on the manner in which it evaporates. As Picknett & Bexon (1977) described in their pioneering work, there are two extreme modes of droplet evaporation, namely the 'constant contact radius' (CR) mode, in which the contact angle $\theta = \theta(t)$ $(0 \leqslant \theta \leqslant \pi)$ decreases with time t but the contact radius $R = R_0$ remains constant, and the 'constant contact angle' (CA) mode, in which the contact radius $R = R(t)$ $(\geqslant 0)$ decreases but the contact angle $\theta = \theta_0$ remains constant; here R_0 and θ_0 denote the initial values of R and θ, respectively.

† Email address for correspondence: s.k.wilson@strath.ac.uk

However, as Picknett & Bexon (1977) also described (and as Bourgès-Monnier & Shanahan (1995) and many other authors have subsequently confirmed), in practice a droplet usually evaporates in what we term a 'stick–slide' (SS) mode, made up of one or more 'stick' phases in which the contact line is pinned (i.e. in which R is constant) and one or more 'slide' phases in which the contact line is de-pinned (i.e. in which R varies). Note that we introduce the term 'stick–slide' (rather than use the term 'stick–slip' introduced by Shanahan (1995) to describe situations in which the 'slip' phases are of relatively short duration compared with the 'stick' phases) to emphasise that in the situations considered in the present work, the 'slip' and 'slide' phases may be of comparable duration. Various SS modes have been observed experimentally, but perhaps the most commonly reported SS mode is one (referred to as the 'combined pinned–receding mode' by Nguyen & Nguyen (2012*b*)) where there is an initial stick phase in which the droplet evaporates in a CR phase, followed by a first slide phase in which the droplet evaporates in a CA phase, followed in turn by a second slide phase in which both R and θ vary simultaneously. In practice, the second slide phase is often of relatively short duration compared with the stick and the first slide phases, in which case it can be neglected when determining the lifetime of the droplet. Thus, in the present work we study a model for the SS mode, sketched in figure 1 (as discussed by, for example, Nguyen & Nguyen (2012*b*), Stauber *et al.* (2013) and Dash & Garimella (2013)), in which initially the droplet evaporates in a CR phase with $R = R_0$ and with $\theta = \theta(t)$ decreasing from $\theta = \theta_0$ $(0 \leqslant \theta_0 \leqslant \pi)$ to the receding contact angle $\theta = \theta^\star$ (referred to as the 'transition contact angle' by Nguyen & Nguyen (2012*b*)) $(0 \leqslant \theta^\star \leqslant \pi)$, after which the droplet evaporates in a CA phase with $\theta = \theta^\star$ and with $R = R(t)$ decreasing from R_0 to zero. The initial CR phase occurs only if $\theta_0 > \theta^\star$; otherwise the contact line is always de-pinned and the droplet simply evaporates in the CA mode. In particular, we verify the model by comparison with the results of relevant physical experiments in the literature and use it to construct a master diagram which shows the relationship between the lifetime of a droplet evaporating in this mode and the lifetimes of initially identical droplets evaporating in the extreme modes for all physically realisable values of the key parameters θ_0 and $\theta^\star$ which characterise the wettability of the system.

2. The diffusion-limited model

In many situations the evaporation of droplets is well described by the diffusion-limited model, in which diffusion of vapour from the droplet into the surrounding atmosphere is the rate-limiting mechanism (see, for example, Picknett & Bexon (1977), Deegan *et al.* (1997), Hu & Larson (2002), McHale *et al.* (2005), Popov (2005), Dunn *et al.* (2009), Kulinich & Farzaneh (2009), Gelderblom *et al.* (2011), Nguyen & Nguyen (2012*a*,*b*), Talbot *et al.* (2012) and Dash & Garimella (2013)).

Assuming that the droplet is sufficiently small that the effect of gravity is negligible, the shape of the droplet will be that of a spherical cap with contact radius $R = R(t)$ $(\geqslant 0)$, contact angle $\theta = \theta(t)$ $(0 \leqslant \theta \leqslant \pi)$ and hence volume $V = V(t)$ $(\geqslant 0)$ given by

$$V = \frac{\pi R^3}{3} \frac{\sin\theta(2+\cos\theta)}{(1+\cos\theta)^2}. \tag{2.1}$$

According to the diffusion-limited model, the rate of change of the droplet volume with respect to time t is

$$\frac{\mathrm{d}V}{\mathrm{d}t} = -\frac{\pi R D(c_{sat} - c_\infty)}{\rho} \frac{g(\theta)}{(1+\cos\theta)^2}, \tag{2.2}$$

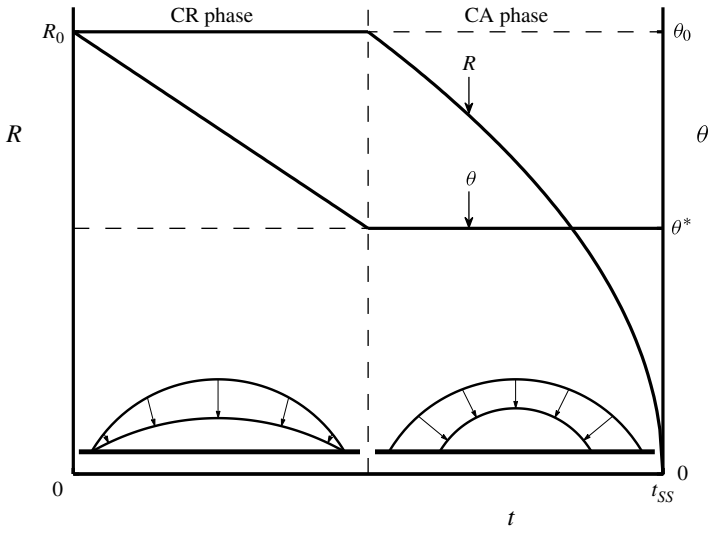

FIGURE 1. Sketch of the SS mode considered in the present work, in which initially the droplet evaporates in a CR phase with $R = R_0$ and with $\theta = \theta(t)$ decreasing from $\theta = \theta_0$ to the receding contact angle $\theta = \theta^\star$, after which the droplet evaporates in a CA phase with $\theta = \theta^\star$ and with $R = R(t)$ decreasing from R_0 to zero.

where D is the diffusion coefficient of vapour in the air, ρ is the density of the fluid, c_{sat} is the vapour concentration at the interface, c_∞ is the vapour concentration far from the interface (which may take values between zero and c_{sat}) and the function $g = g(\theta)$ is given by

$$g(\theta) = (1+\cos\theta)^2 \left\{ \tan\left(\frac{\theta}{2}\right) + 8\int_0^\infty \frac{\cosh^2(\theta\tau)}{\sinh(2\pi\tau)} \tanh[\tau(\pi-\theta)]\,\mathrm{d}\tau \right\} \tag{2.3}$$

(see, for example, Popov (2005)). Note that $g(0) = 16/\pi$, $g(\pi/2) = 2$ and $g \sim (\pi - \theta)^3 \log 2 \to 0^+$ as $\theta \to \pi^-$.

3. Theoretical predictions for the lifetimes of droplets

The lifetime of an evaporating droplet is the time it takes for its volume V to reach zero. Depending on the manner in which the droplet evaporates, within the present model its volume V will reach zero when its radius R and/or its contact angle θ reaches zero, and so the lifetime of a droplet is obtained by integrating (2.2) with respect to t until either $R = 0$ or $\theta = 0$, as appropriate. Hence, upon scaling t with an appropriate reference time scale,

$$\frac{\rho}{2D(c_{sat}-c_\infty)}\left(\frac{3V_0}{2\pi}\right)^{2/3}, \tag{3.1}$$

where V_0 is the initial value of V, the lifetime of a droplet evaporating in the CR mode, denoted by $t_{CR} = t_{CR}(\theta_0)$, is given by

$$t_{CR} = \left(\frac{2(1+\cos\theta_0)^2}{\sin\theta_0(2+\cos\theta_0)}\right)^{2/3} \int_0^{\theta_0} \frac{2\,\mathrm{d}\theta}{g(\theta)}, \tag{3.2}$$

and the lifetime of a droplet evaporating in the CA mode, denoted by $t_{CA} = t_{CA}(\theta_0)$, is given by

$$t_{CA} = \left(\frac{2(1+\cos\theta_0)^2}{\sin\theta_0(2+\cos\theta_0)} \right)^{2/3} \frac{\sin\theta_0(2+\cos\theta_0)}{g(\theta_0)}. \tag{3.3}$$

The lifetime of a droplet evaporating in the SS mode is denoted by $t_{SS} = t_{SS}(\theta_0, \theta^\star)$; unlike t_{CR} and t_{CA}, it is in general a function of the receding contact angle $\theta^\star$ as well as of the initial contact angle θ_0 and will not, in general, be equal to either t_{CR} or t_{CA} when $\theta_0 > \theta^\star$. Specifically, for $0 \leqslant \theta_0 \leqslant \theta^\star$, the droplet simply evaporates in the CA mode, and hence we have $t_{SS} = t_{CA}$, where t_{CA} is given by (3.3); but for $\theta_0 \geqslant \theta^\star$, initially the droplet evaporates in a CR phase until θ reaches $\theta^\star$, after which it evaporates in a CA phase until R reaches zero, and hence we have

$$t_{SS} = \left(\frac{2(1+\cos\theta_0)^2}{\sin\theta_0(2+\cos\theta_0)} \right)^{2/3} \left[\int_{\theta^*}^{\theta_0} \frac{2\,\mathrm{d}\theta}{g(\theta)} + \frac{\sin\theta^*(2+\cos\theta^*)}{g(\theta^*)} \right], \tag{3.4}$$

where the first term on the right-hand side of (3.4) represents the duration of the CR phase and the second term represents the duration of the CA phase.

4. Experimental validation of the model

Before analysing the theoretically predicted lifetime of an evaporating droplet, t_{SS}, given by (3.4), the model is verified by comparison with the results of relevant physical experiments in the literature for which all of the necessary data are available. In particular, we use the 29 sets of experimental results for droplets evaporating in a SS mode obtained by Bourgès-Monnier & Shanahan (1995), Uno *et al.* (1998), Fukai *et al.* (2006), Li *et al.* (2009), Song *et al.* (2011), Nguyen *et al.* (2012), Lim *et al.* (2012), Yu, Wang & Zhao (2012) and Dash & Garimella (2013) for which the duration of the second slide phase was at most 10 % of the lifetime of the droplet. For each of these sets of experimental results, the experimentally determined lifetime of the droplet, denoted by t_{exp}, was obtained by fitting the experimental data for $V^{2/3}$ as a linear function of t and extrapolating to $V = 0$ (which is, of course, exact only for the CA mode) as proposed by, for example, Nguyen *et al.* (2012). Figure 2 shows t_{SS} calculated numerically from (3.4) using the experimentally determined values of θ_0 and $\theta^\star$ plotted as a function of the corresponding values of t_{exp}, together with a solid line showing $t_{SS} = t_{exp}$ and dashed lines showing 5 and 10 % deviations from $t_{SS} = t_{exp}$. In particular, figure 2 shows that the theoretically predicted values are in excellent agreement with the experimentally determined values, with all of the values of t_{SS} lying within 10 % of t_{exp} and 26 of the 29 values lying within 5 %. Details of the sets of experimental results used in figure 2 (and subsequently in figure 5) are given in table 1.

5. Results

5.1. *The lifetimes of evaporating droplets*

Figures 3 and 4 show the lifetime of a droplet evaporating in the SS mode, t_{SS}, given by (3.4), together with the lifetimes of initially identical droplets evaporating in the CR and CA modes, t_{CR} and t_{CA}, given by (3.2) and (3.3), plotted as functions of θ_0 for various values of $\theta^\star$ in the ranges $0 < \theta^\star \leqslant \pi/2$ and $\pi/2 \leqslant \theta^\star < \pi$, respectively.

https://doi.org/10.1017/jfm.2014.94 Published online by Cambridge University Press

Reference	Figure	Fluid	Substrate
Bourgès-Monnier & Shanahan (1995)	Figure 1 (stages II–IV)	Water	Polished epoxy resin
	Figure 2 (stages II–IV)	Water	Polished epoxy resin
Uno *et al.* (1998)	Figure 3(*d*)	Latex dispersion	$ODTES_{100}$ on glass
Fukai *et al.* (2006)	Figure 3	Water	SO_3H on silicon
	Figure 4	Water	SO_3H on silicon
	Figure 5	Xylene	R_f on silicon
Li *et al.* (2009)	Figure 5 (all nine sets)	Water	Dialkyl disulfides on gold-covered mica
Song *et al.* (2011)	Figure 2	Water	Platinum
Nguyen *et al.* (2012)	Figure 5 (all four sets)	Water	Oct-silicon
	Figure 9(*a*)	Water	Oct-silicon
	Figure 9(*b*)	Water	OTS-silicon
	Figure 9(*c*)	Water	Teflon
Lim *et al.* (2012)	Figure 4(*c*)	Water	Pyrex glass
	Figure 6(*b*)	Diethylene glycol with coffee particles	Pyrex glass
Yu *et al.* (2012)	Figures 2 and 4 (2 μl droplet)	Water	Teflon on PDMS on glass
Dash & Garimella (2013)	Figure 3 and table 3 (all three sets)	Water	Teflon on silicon

TABLE 1. Details of the 29 sets of experimental results used in figures 2 and 5. In the 'Substrate' column, '$ODTES_{100}$' denotes octadecyltriethoxysilane with a static contact angle of roughly 100° for pure water, 'SO_3H' denotes 3-mercaptopropyltrimethoxysilane, 'R_f' denotes perfluorohexylethyltrimethoxysilane, 'Oct-silicon' denotes silicon hydrophobised with octanol, 'OTS-silicon' denotes silicon hydrophobised with *n*-octadecyltrichlorosilane in heptane, and 'PDMS' denotes polydimethylsiloxane.

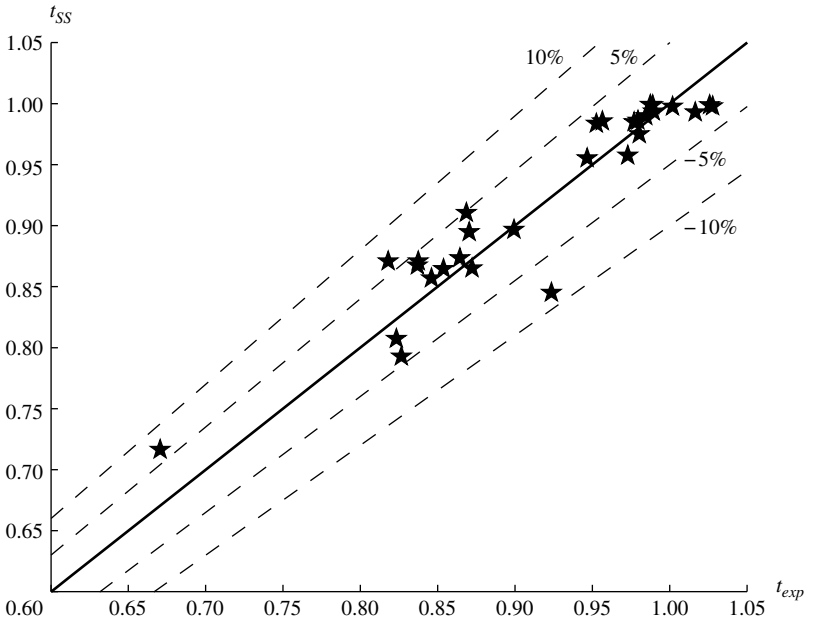

FIGURE 2. The theoretically predicted lifetimes of evaporating droplets, t_{SS}, calculated numerically from (3.4) using the experimentally determined values of θ_0 and $\theta^\star$, plotted as a function of the corresponding experimentally determined values, t_{exp}, together with a solid line showing $t_{SS} = t_{exp}$ and dashed lines showing 5 and 10 % deviations from $t_{SS} = t_{exp}$.

Figures 3 and 4 show that $t_{CR} < t_{CA}$ when $0 < \theta_0 < \theta_{crit}$, where $\theta_0 = \theta_{crit} \simeq 2.5830$ (i.e. $\theta_{crit} \simeq 148°$), but $t_{CR} > t_{CA}$ when $\theta_{crit} < \theta_0 < \pi$, with $t_{CR} = t_{CA} = t_{SS} = 0$ at $\theta_0 = 0$, $t_{CR} = t_{CA} \simeq 0.9354$ at $\theta_0 = \theta_{crit}$ and $t_{CR} = t_{CA} = t_{SS} = (4^{1/3} \log 2)^{-1} \simeq 0.9088$ at $\theta_0 = \pi$. In particular, figures 3 and 4 illustrate the sometimes overlooked result first obtained qualitatively by Picknett & Bexon (1977) that a droplet evaporating in the CR mode has a shorter lifetime than an initially identical droplet evaporating in the CA mode when $0 < \theta_0 < \theta_{crit}$, but that the opposite is true when $\theta_{crit} < \theta_0 < \pi$, and that in the special case $\theta_0 = \pi$ the CR, CA and SS modes all coincide (i.e. $R \equiv R_0 = 0$ and $\theta \equiv \theta_0 = \pi$ for all t). The maximum value of $t_{CR} \simeq 0.9354$ occurs at $\theta_0 = \theta_{crit}$, and the maximum value of $t_{CA} = 1$ occurs at $\theta_0 = \pi/2$. The maximum value of t_{SS} depends on the value of $\theta^\star$: when $0 \leqslant \theta^\star \leqslant \pi/2$ it occurs at $\theta_0 = \hat{\theta}_0$, where $\hat{\theta}_0 = \hat{\theta}_0(\theta^\star)$ is the unique value of θ_0 in the range $\pi/2 \leqslant \theta_0 \leqslant \theta_{crit}$ at which $t_{SS} = t_{CA}$, indicated with solid dots in figure 3(*b*); but when $\pi/2 \leqslant \theta^\star \leqslant \pi$ it always occurs at $\theta_0 = \pi/2$, at which $t_{SS} = t_{CA} = 1$.

Since the SS mode is a simple combination of the extreme modes, it would be natural to assume, as some previous authors (such as Nguyen & Nguyen (2012*b*)) have done, that the lifetime of a droplet evaporating in this mode is always constrained by the lifetimes of initially identical droplets evaporating in the extreme modes. However, while figures 3 and 4 show that when $0 < \theta_0 \leqslant \pi/2$ (and, in particular, in the thin-film limit $\theta_0 \to 0^+$) it is indeed correct that t_{SS} lies between t_{CR} and t_{CA}, they also show that when $\pi/2 < \theta_0 < \pi$ this result is not, in general, correct. Specifically, figures 3 and 4 show that $t_{SS} > \max(t_{CR}, t_{CA})$ when θ_0 lies in the range $\hat{\theta}_0 < \theta_0 < \pi$ in the case $0 < \theta^\star \leqslant \pi/2$ and when θ_0 lies in the range $\theta^\star < \theta_0 < \pi$

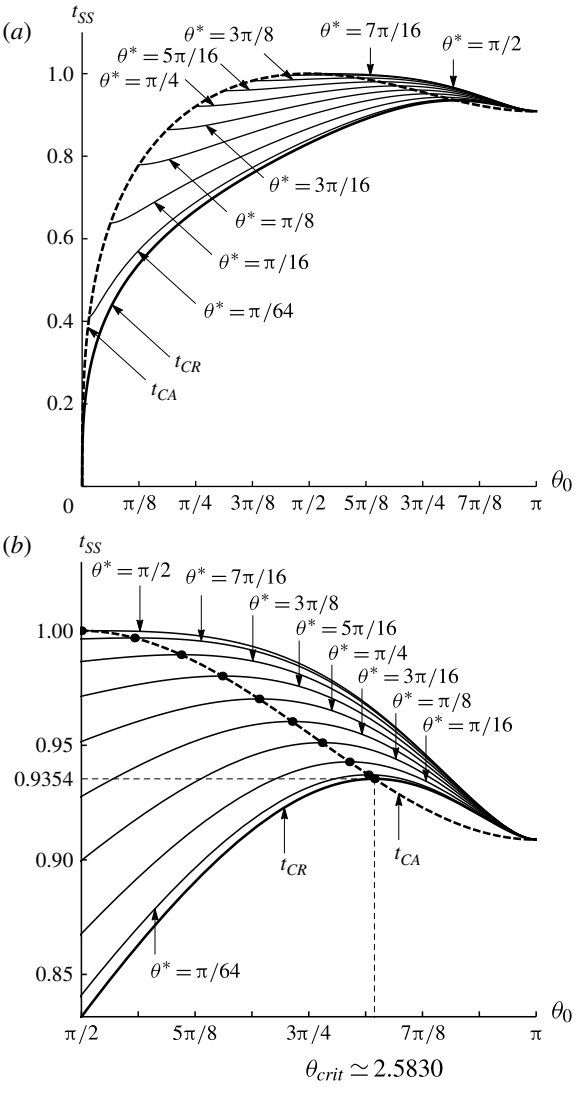

FIGURE 3. The lifetime of a droplet evaporating in the SS mode, t_{SS}, given by (3.4), plotted as a function of the initial contact angle θ_0 for various receding contact angles in the range $0 < \theta^\star \leqslant \pi/2$, namely $\theta^\star = \pi/64,\ \pi/16,\ \pi/8,\ 3\pi/16,\ \pi/4,\ 5\pi/16,\ 3\pi/8,\ 7\pi/16$ and $\pi/2$, together with the lifetimes of initially identical droplets evaporating in the CR and CA modes, t_{CR} and t_{CA}, given by (3.2) and (3.3), respectively. The behaviour in the range $\pi/2 \leqslant \theta_0 \leqslant \pi$ is shown in greater detail in (*b*), where the values of $\theta_0 = \hat{\theta}_0$ at which the maximum value of t_{SS} occurs are indicated with solid dots.

in the case $\pi/2 \leqslant \theta^\star < \theta_{crit}$. In other words, when $0 < \theta^\star < \theta_{crit}$ (but not otherwise), the lifetime of a droplet evaporating in the SS mode is longer than the lifetimes of initially identical droplets evaporating in the extreme modes for sufficiently large values of θ_0. Furthermore, figures 3 and 4 also show that for any value of $\theta^\star$, $t_{CR}, t_{CA}, t_{SS} \leqslant t_{CA}(\pi/2) = 1$, i.e. the longest lifetime of any droplet evaporating in any of the three modes for all possible values of θ_0 and $\theta^\star$ is that of a droplet with initial

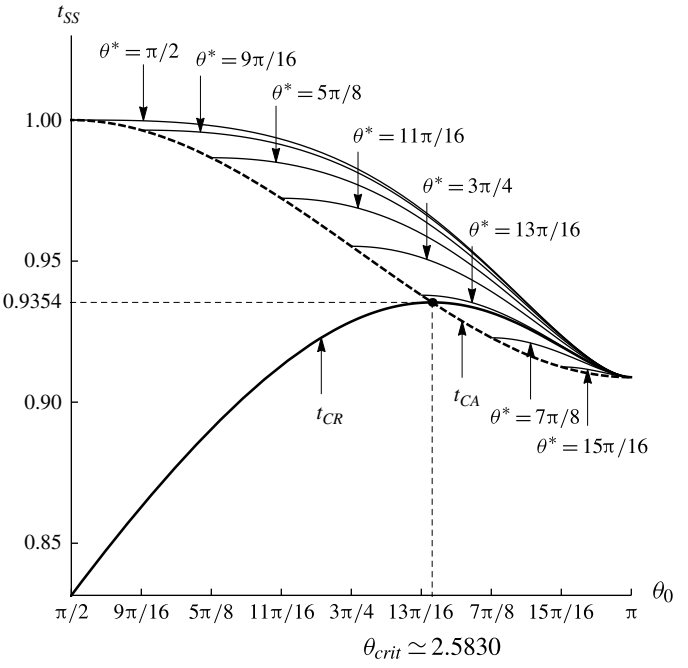

FIGURE 4. As figure 3, except for various receding contact angles in the range $\pi/2 \leqslant \theta^\star < \pi$, namely $\theta^\star = \pi/2, 9\pi/16, 5\pi/8, 11\pi/16, 3\pi/4, 13\pi/16\,(< \theta_{crit} \simeq 2.5830)$, $7\pi/8\,(> \theta_{crit})$ and $15\pi/16$. For clarity, only the behaviour in the range $\pi/2 \leqslant \theta_0 \leqslant \pi$ is shown.

contact angle $\theta_0 = \pi/2$ evaporating in the CA mode. Note that the behaviour of the curves corresponding to t_{SS} is qualitatively different from that tentatively suggested by Shanahan, Sefiane & Moffat (2011). Details of the behaviour of t_{CR}, t_{CA} and t_{SS} in appropriate asymptotic limits are given in the next subsection.

5.2. *Asymptotic behaviour of t_{CR}, t_{CA} and t_{SS}*

As figure 3 shows, in the limit of small initial contact angle, $\theta_0 \to 0^+$, the curves corresponding to t_{CR} and t_{CA} approach zero from above with infinite slope according to

$$t_{CR} = \left(\frac{1}{3}\right)^{2/3} \frac{\pi}{2}\,\theta_0^{1/3} + O\left(\theta_0^{4/3}\right) \tag{5.1}$$

and

$$t_{CA} = \left(\frac{1}{3}\right)^{2/3} \frac{3\pi}{4}\,\theta_0^{1/3} + O\left(\theta_0^{4/3}\right) \tag{5.2}$$

(and hence $t_{CA} = 3t_{CR}/2$ at leading order in this limit); in the limit of large initial contact angle, $\theta_0 \to \pi^-$, the curves corresponding to t_{CR} and t_{CA} approach the value $(4^{1/3}\log 2)^{-1} \simeq 0.9088$ from above with zero slope according to

$$t_{CR} = \frac{1}{4^{1/3}\log 2}\left[1 - \frac{4\log 2 - 1}{12\log 2}(\pi - \theta_0)^2 \log(\pi - \theta_0)\right] + O\left(\pi - \theta_0\right)^2 \tag{5.3}$$

and

$$t_{CA} = \frac{1}{4^{1/3}\log 2}\left[1 + \frac{4\log 2 - 1}{24\log 2}(\pi - \theta_0)^2\right] + O\left(\pi - \theta_0\right)^4. \tag{5.4}$$

As figures 3 and 4 show, for all values of $\theta^\star$, the curves corresponding to t_{SS} depart from the curve corresponding to t_{CA} at $\theta_0 = \theta^\star$ with zero slope according to

$$t_{SS} = t_{CA}(\theta^\star) + A(\theta^\star)(\theta_0 - \theta^\star)^2 + O\left(\theta_0 - \theta^\star\right)^3 \tag{5.5}$$

in the limit $\theta_0 \to \theta^{\star+}$, where the coefficient $A = A(\theta^\star)$ is given by

$$A(\theta^\star) = \left(\frac{2(1+\cos\theta^\star)^2}{\sin\theta^\star(2+\cos\theta^\star)}\right)^{2/3} \times \frac{(2\cos^2\theta^\star + 2\cos\theta^\star - 3)g(\theta^\star) - \sin\theta^\star(2+\cos\theta^\star)g'(\theta^\star)}{\sin\theta^\star(2+\cos\theta^\star)g(\theta^\star)^2}, \tag{5.6}$$

with a dash ($'$) denoting differentiation with respect to argument. In particular, since $A > 0$ for $0 < \theta^\star < \pi/2$ but $A < 0$ for $\pi/2 < \theta^\star < \pi$, the curves corresponding to t_{SS} have a local minimum at $\theta_0 = \theta^\star$ for $0 < \theta^\star < \pi/2$ as shown in figure 3(*a*), but a local maximum at $\theta_0 = \theta^\star$ for $\pi/2 < \theta^\star < \pi$ as shown in figure 4. Furthermore, in the limit of large initial contact angle, $\theta_0 \to \pi^-$, the curves corresponding to t_{SS} approach the value $(4^{1/3}\log 2)^{-1} \simeq 0.9088$ with zero slope according to (5.3) to the order of accuracy shown.

As figure 3 shows, in the limit of small receding contact angle, $\theta^\star \to 0^+$, the curves corresponding to t_{SS} approach the curve corresponding to t_{CR} from above for all values of θ_0 according to

$$t_{SS} = t_{CR}(\theta_0) + \left(\frac{2(1+\cos\theta_0)^2}{\sin\theta_0(2+\cos\theta_0)}\right)^{2/3}\frac{\pi}{16}\theta^\star + O\left(\theta^{\star 2}\right). \tag{5.7}$$

As figure 4 shows, in the limit of large receding contact angle, $\theta^\star \to \pi^-$, the curves corresponding to t_{SS} approach the curve corresponding to t_{CA} from above for all values of θ_0 in the vanishingly small range $\theta^\star < \theta_0 < \pi$ according to

$$t_{SS} = \frac{1}{4^{1/3}\log 2}\left[1 + \frac{4\log 2 - 1}{24\log 2}(\pi - \theta_0)^2\left\{1 - 2\log\left(\frac{\pi - \theta_0}{\pi - \theta^\star}\right)\right\}\right] + O\left(\pi - \theta_0\right)^4. \tag{5.8}$$

5.3. *Master diagram*

The relationship between the lifetimes of initially identical droplets evaporating in the three different modes is summarised in the master diagram presented in figure 5, which shows how the θ_0–$\theta^\star$ parameter plane is divided up into regions in which the six possible orderings of t_{CR}, t_{CA} and t_{SS} occur. Specifically, region I corresponds to $t_{CR} < t_{SS} < t_{CA}$, region II to $t_{CR} < t_{CA} < t_{SS}$, region III to $t_{CA} < t_{CR} < t_{SS}$, region IV to $t_{CA} < t_{SS} < t_{CR}$, region V to $t_{SS} = t_{CA} < t_{CR}$ and region VI to $t_{CR} < t_{SS} = t_{CA}$. In particular, figure 5 shows that these are the only possible orderings that can occur. For example, there are no parameter values for which $t_{SS} < \min(t_{CR}, t_{CA})$, i.e. the lifetime of a droplet evaporating in the SS mode can never be less than both of the lifetimes

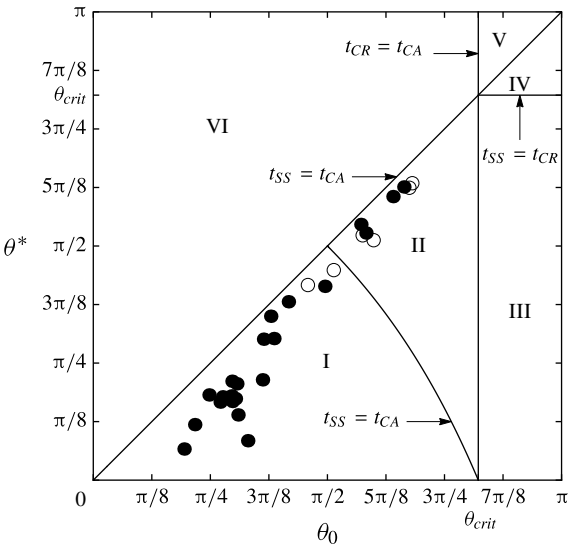

FIGURE 5. Master diagram showing how the θ_0–$\theta^\star$ parameter plane is divided up into regions in which the six possible orderings of the lifetimes of initially identical droplets evaporating in the CR, CA and SS modes occur. Region I corresponds to $t_{CR} < t_{SS} < t_{CA}$, region II to $t_{CR} < t_{CA} < t_{SS}$, region III to $t_{CA} < t_{CR} < t_{SS}$, region IV to $t_{CA} < t_{SS} < t_{CR}$, region V to $t_{SS} = t_{CA} < t_{CR}$ and region VI to $t_{CR} < t_{SS} = t_{CA}$. In particular, note that $t_{SS} > \max(t_{CR}, t_{CA})$ in regions II and III. For each set of experimental results, the appropriate point is denoted by a solid circle if the experimentally determined lifetime of the droplet, t_{exp}, is correctly ordered with respect to the theoretically predicted values of t_{CR} and t_{CA}, and by an open circle if it is not.

of initially identical droplets evaporating in the extreme modes. The upper left-hand half of the parameter plane (i.e. regions V and VI), $\theta_0 > \theta^\star$, corresponds to situations in which the SS and CA modes coincide, and so, in particular, the behaviour in it is independent of $\theta^\star$. The most interesting behaviour occurs in the lower right-hand half of the parameter plane (i.e. regions I–IV), $\theta_0 < \theta^\star$, in which the SS mode has both a CR and a CA phase. In particular, approximately 53 % of it is occupied by regions II and III in which $t_{SS} > \max(t_{CR}, t_{CA})$, i.e. in which the lifetime of a droplet evaporating in the SS mode is longer than the lifetimes of initially identical droplets evaporating in the extreme modes.

Figure 5 also includes points corresponding to the 29 sets of experimental results shown previously in figure 2. Note that since all of these sets of experimental results include the initial CR phase, they all have $\theta_0 > \theta^\star$, and hence all of the points lie in the lower right-hand half of the parameter plane. In particular, for each set of experimental results the appropriate point in the θ_0–$\theta^\star$ parameter plane is denoted by a solid circle if the experimentally determined lifetime of the droplet, t_{exp}, is correctly ordered with respect to the theoretically predicted values of t_{CR} and t_{CA}, and by an open circle if it is not. As figure 5 shows, all of the points are in regions I and II, and 23 of the 29 sets of experimental results are correctly ordered, providing encouraging support for the present model. However, note that since all of the sets of experimental results shown correspond to values of θ_0 satisfying $\theta_0 < \theta_{crit}$, there are no points in regions III and IV, and so testing the present model for superhydrophobic droplets with $\theta_0 > \theta_{crit}$ remains an open challenge.

6. Conclusions

In the present work we obtained the complete description of the unexpectedly subtle relationship between the lifetime of a droplet on a solid substrate evaporating in a SS mode and the lifetimes of initially identical droplets evaporating in the extreme modes, which is summarised in the master diagram presented in figure 5. In particular, we showed that the lifetime of a droplet is not, in general, constrained by the lifetimes of the extreme modes.

Acknowledgements

The first author (JMS) gratefully acknowledges the financial support of the UK Engineering and Physical Sciences Research Council (EPSRC), the University of Strathclyde and the University of Edinburgh via a postgraduate research studentship. This work was begun while the second author (SKW) was a Visiting Fellow at the Isaac Newton Institute for Mathematical Sciences in Cambridge, UK, as part of the programme on 'Mathematical Modelling and Analysis of Complex Fluids and Active Media in Evolving Domains' and completed while he was a Leverhulme Trust Research Fellow (2013–2015) supported by award RF-2013-355.

References

BOURGÈS-MONNIER, C. & SHANAHAN, M. E. R. 1995 Influence of evaporation on contact angle. *Langmuir* **11**, 2820–2829.

CAZABAT, A.-M. & GUÉNA, G. 2010 Evaporation of macroscopic sessile droplets. *Soft Matt.* **6**, 2591–2612.

DASH, S. & GARIMELLA, S. V. 2013 Droplet evaporation dynamics on a superhydrophobic surface with negligible hysteresis. *Langmuir* **29**, 10785–10795.

DEEGAN, R. D., BAKAJIN, O., DUPONT, T. F., HUBER, G., NAGEL, S. R. & WITTEN, T. A. 1997 Capillary flow as the cause of ring stains from dried liquid drops. *Nature* **389**, 827–829.

DUNN, G. J., WILSON, S. K., DUFFY, B. R., DAVID, S. & SEFIANE, K. 2009 The strong influence of substrate conductivity on droplet evaporation. *J. Fluid Mech.* **623**, 329–351.

ERBIL, H. Y. 2012 Evaporation of pure liquid sessile and spherical suspended drops: a review. *Adv. Colloid Interface Sci.* **170**, 67–86.

FUKAI, J., ISHIZUKA, H., SAKAI, Y., KANEDA, M., MORITA, M. & TAKAHARA, A. 2006 Effects of droplet size and solute concentration on drying process of polymer solution droplets deposited on homogeneous surfaces. *Intl J. Heat Mass Transfer* **49**, 3561–3567.

GELDERBLOM, H., MARÍN, Á. G., NAIR, H., VAN HOUSELT, A., LEFFERTS, L., SNOEIJER, J. H. & LOHSE, D. 2011 How water droplets evaporate on a superhydrophobic substrate. *Phys. Rev.* E **83**, 026306.

HU, H. & LARSON, R. G. 2002 Evaporation of a sessile droplet on a substrate. *J. Phys. Chem.* B **106**, 1334–1344.

KULINICH, S. A. & FARZANEH, M. 2009 Effect of contact angle hysteresis on water droplet evaporation from super-hydrophobic surfaces. *Appl. Surf. Sci.* **255**, 4056–4060.

LI, G., FLORES, S. M., VAVILALA, C., SCHMITTEL, M. & GRAF, K. 2009 Evaporation dynamics of microdroplets on self-assembled monolayers and dialkyl disulfides. *Langmuir* **25**, 13438–13447.

LIM, T., YANG, J., LEE, S., CHUNG, J. & HONG, D. 2012 Deposit pattern of inkjet printed pico-liter droplet. *Intl J. Precis. Engng Manuf.* **13**, 827–833.

MCHALE, G., AQIL, S., SHIRTCLIFFE, N. J., NEWTON, M. I. & ERBIL, H. Y. 2005 Analysis of droplet evaporation on a superhydrophobic surface. *Langmuir* **21**, 11053–11060.

NGUYEN, T. A. H. & NGUYEN, A. V. 2012*a* On the lifetime of evaporating sessile droplets. *Langmuir* **28**, 1924–1930.

NGUYEN, T. A. H. & NGUYEN, A. V. 2012*b* Increased evaporation kinetics of sessile droplets by using nanoparticles. *Langmuir* **28**, 16725–16728.

NGUYEN, T. A. H., NGUYEN, A. V., HAMPTON, M. A., XU, Z. P., HUANG, L. & RUDOLPH, V. 2012 Theoretical and experimental analysis of droplet evaporation on solid surfaces. *Chem. Engng Sci.* **69**, 522–529.

PICKNETT, R. G. & BEXON, R. 1977 The evaporation of sessile or pendant drops in still air. *J. Colloid Interface Sci.* **61**, 336–350.

POPOV, Y. O. 2005 Evaporative deposition patterns: spatial dimensions of the deposit. *Phys. Rev.* E **71**, 036313.

SHANAHAN, M. E. R. 1995 Simple theory of 'stick–slip' wetting hysteresis. *Langmuir* **11**, 1041–1043.

SHANAHAN, M. E. R., SEFIANE, K. & MOFFAT, J. R. 2011 Dependence of volatile droplet lifetime on the hydrophobicity of the substrate. *Langmuir* **27**, 4572–4577.

SONG, H., LEE, Y., JIN, S., KIM, H.-Y. & YOO, J. Y. 2011 Prediction of sessile drop evaporation considering surface wettability. *Microelectron. Engng* **88**, 3249–3255.

STAUBER, J. M., WILSON, S. K., DUFFY, B. R. & SEFIANE, K. 2013 Comment on "Increased evaporation kinetics of sessile droplets by using nanoparticles". *Langmuir* **29**, 12328–12329.

TALBOT, E. L., BERSON, A., BROWN, P. S. & BAIN, C. D. 2012 Evaporation of picoliter droplets on surfaces with a range of wettabilities and thermal conductivities. *Phys. Rev.* E **85**, 061604.

UNO, K., HAYASHI, K., HAYASHI, T., ITO, K. & KITANO, H. 1998 Particle adsorption in evaporating droplets of polymer latex dispersions on hydrophilic and hydrophobic surfaces. *Colloid Polym. Sci.* **276**, 810–815.

YU, Y.-S., WANG, Z. & ZHAO, Y.-P. 2012 Experimental and theoretical investigations of evaporation of sessile water droplet on hydrophobic surfaces. *J. Colloid Interface Sci.* **365**, 254–259.